Optimum phase for rugate filter synthesis by Fourier transforms

Verly, Pierre G.

Publisher's version / Version de l'éditeur:
https://doi.org/10.1364/AO.50.00C124
Applied Optics, 50, 9, pp. C124-C128, 2010-11-15

Optimum phase for rugate filter synthesis by Fourier transforms

Pierre G. Verly

Institute for Microstructural Sciences, National Research Council of Canada, 1200 Montreal Road, Ottawa, Ontario K1A 0R6, Canada (Pierre.Verly@nrc-cnrc.gc.ca)

Received 2 August 2010; accepted 21 September 2010;
posted 5 October 2010 (Doc. ID 132571); published 15 November 2010

An optimum phase is developed for the synthesis of rugate reflectors by a simple Fourier transform. This phase belongs to a complex function of the desired spectral characteristics and is usually a free parameter. In general, it receives much less attention than the function magnitude, which is not known exactly. The current work shows that phase shaping alone produces surprisingly good results and has other advantages in rugate filter synthesis. In addition, the operating mode of this design procedure is quite unusual and interesting in itself.

OCIS codes: 310.0310, 310.1620, 310.5696, 310.6805, 120.2440, 350.2460.

1. Introduction

Thin-film synthesis techniques typically generate solutions from much more elementary starting designs than conventional refinement. There are many situations where this is an appreciable advantage. One of the first practical synthesis approaches, proposed several decades ago but still of interest, in particular for rugate filters (also known as inhomogeneous or graded-index filters), establishes an analytical relationship between a refractive-index profile $n(x)$ and its transmittance $T(\sigma)$ through a Fourier transform (FT) [1–3]:

$$\ln\left(\frac{n(x)}{n_0}\right) \overset{\text{FT}}{\leftrightarrow} \frac{i}{\pi}\frac{\tilde{Q}(T,\sigma)}{\sigma}. \tag{1a}$$

In this relation,

$$\tilde{Q}(T,\sigma) = Q(T)\exp[i\phi(\sigma)] \tag{1b}$$

is a complex function known as the Q function, x is twice the centered optical thickness (see the figures), n_0 is a constant used to center $n(x)$ in the specified index range, and $\sigma = 1/\lambda$ is the wavenumber or inverse wavelength. In principle, losses and dispersion are ignored, but there are indirect ways of getting around this limitation [4–7].

Unfortunately, the analytical forms of the Q magnitude $Q(T)$ proposed in the literature lose their accuracy as the reflectance $R = 1 - T$ increases. Q is approximately equal to $\sqrt{R}$ when R is small. The Q phase $\phi(\sigma)$ is usually unknown and has to be generated in the synthesis process—a degree of freedom that can be exploited. Additional errors are often introduced, for example, when $n(x)$ is forced to fit within prescribed thickness and refractive-index limits.

Most of the efforts made to improve the accuracy of the Q function concentrate on its magnitude [8–13]. The phase is usually a secondary concern, except (i) in rare situations where it is specified [14], (ii) to ensure that iterative numerical corrections made to the Q function are constructive [11,12], or (iii) to control the shape of the refractive-index profile—an important consideration when there are index and/or thickness constraints [11,12,15,16]. Multiple filter solutions of essentially the same reflectance in the region of interest but different phases are usually possible, from which the most suitable for fabrication can be selected.

This work concentrates on the phase $\phi(\sigma)$ for the design of rugate reflectors. Because the reflectance of such filters is typically concentrated in the spectral region of interest, it is possible to simplify the

0003-6935/11/09C124-05$15.00/0

previous approaches [11,12] and directly use Eq. (1) in the synthesis. It is shown that surprisingly good results are possible by properly shaping $\phi(\sigma)$, while $Q(T)$ is fixed and takes published analytical forms. The accuracy of $Q(T)$ is not critical. Furthermore, this design procedure has other useful characteristics and an unusual, quite interesting operating mode.

2. Theory

An interesting phase first applied to thin films by Druessel *et al.* and recently used by Cheng *et al.* for the design and fabrication of rather elaborate rugate filters is known as the SWIFT phase [13,17]:

$$\frac{\phi(\sigma)}{2\pi} = \frac{x_1 - x_0}{\int_0^\infty \left|\frac{Q(T)}{\nu}\right|^2 \mathrm{d}\nu} \int_0^\sigma \int_0^\eta \left|\frac{Q(T)}{\nu}\right|^2 \mathrm{d}\nu \mathrm{d}\eta + x_0\sigma. \quad (2)$$

Here x_0 and x_1 are symmetrical thickness limits defining a region where, in principle, the amplitude of the refractive-index modulation is approximately uniform. The slope $d\phi/d\sigma$ is gradually adjusted so that different spectral regions are mapped to different regions of the index profile. The index regions are progressively shifted along the thickness axis to prevent overlaps and excessive refractive-index buildup (tilting the phase shifts $n(x)$ in the x direction). This works well for chirped wide-band reflectors but less so for narrow bands because their contribution to the index profile must be thick and of low contrast. It is, therefore, more difficult to avoid the overlap of refractive-index contributions from different parts of the spectrum.

Figure 1 illustrates an FT design obtained from Eqs. (1) and (2) and the Q function [8,10]:

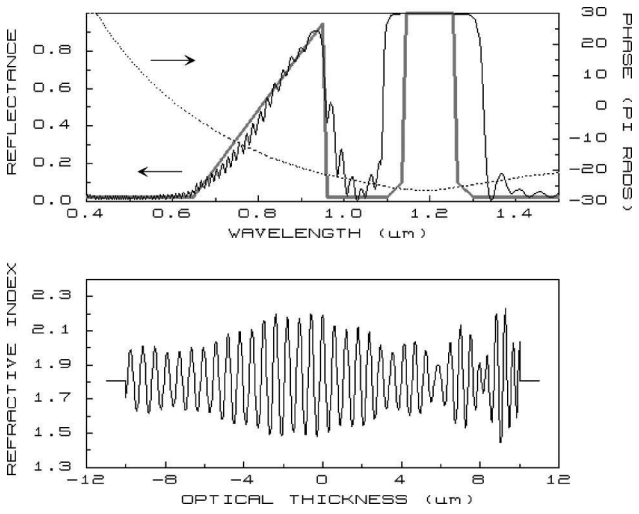

Fig. 1. Fourier transform design of a rugate reflector obtained from Eqs. (1)–(3): thick gray line, reflectance target; dotted black line, SWIFT phase; solid black lines, calculated refractive-index profile and reflectance.

$$Q(T) = \ln\left(\sqrt{\frac{1}{T}} - \sqrt{\frac{1}{T} - 1}\right). \quad (3)$$

The factor $x_1 - x_0$ in Eq. (2) is set to the system's x thickness or twice its optical thickness. In principle, this should be the region, controlled through the SWIFT phase curvature, where the refractive-index modulation is approximately uniform. The SWIFT phase is represented by a dotted black line in the figure. The spectral target depicted by a thick gray line consists of a linear ramp from 2% to 95% reflectance and a narrow band of 99.9% reflectance (which is high for the FT method). Elsewhere in the region of interest, the reflectance must be less than 2%. Light is at normal incidence. The refractive-index profile represented in the lower part of the figure has an optical thickness of 20 μm, essentially what is needed for the narrow reflectance band alone. For simplicity, the system is immersed in a medium of average index (1.8). The refractive-index limits are 1.45 and 2.25.

The index profile is chirped and relatively well distributed in the prescribed thickness and refractive-index spaces. The calculated reflectance is reasonable considering the simplicity of the calculation and the expected limitations for narrow bands and high reflectance. The beats in the index profile reveal that the contributions of the two reflectance bands overlap, which is not surprising.

The solution is greatly improved when the SWIFT phase is optimized. This is an interesting exercise which is not as simplistic as it may seem. Good routines are essential. In this work, the optimization is performed with an upgraded version of the approach described in [11,12]. The numerical gradients are replaced by analytical gradients of the following type:

$$\partial M/\partial\phi_k = \sum_i \partial M/\partial n_i \partial n_i/\partial\phi_k \qquad i,k = 1,2,\ldots, \quad (4)$$

where M is a standard merit function characterizing the root-mean-squared reflectance error (desired–calculated); $n_i = n(x_i)$ and are points on the x and σ grids used in the calculations; $\partial n/\partial\phi$ is obtained from Eq. (1) and $\partial M/\partial n$ is an analytical gradient described in [18]. A quasi-Newton algorithm minimizes the merit value by varying the phase. A Levenberg–Marquardt algorithm based on a similar transmittance gradient $\partial T/\partial\phi_k$ is also available. The Q-function magnitude can be refined in the same way as the phase. Analytical gradients and the way they are calculated make a significant difference in terms of accuracy and computation speed [18].

3. Numerical Results

Figure 2 illustrates the result of the SWIFT phase optimization. The reflectance is considerably improved, in particular in the narrow band. The refractive-index contrast is reduced and better distributed. The Q phase has ripples and a stronger curvature across the 2nd reflectance band. This

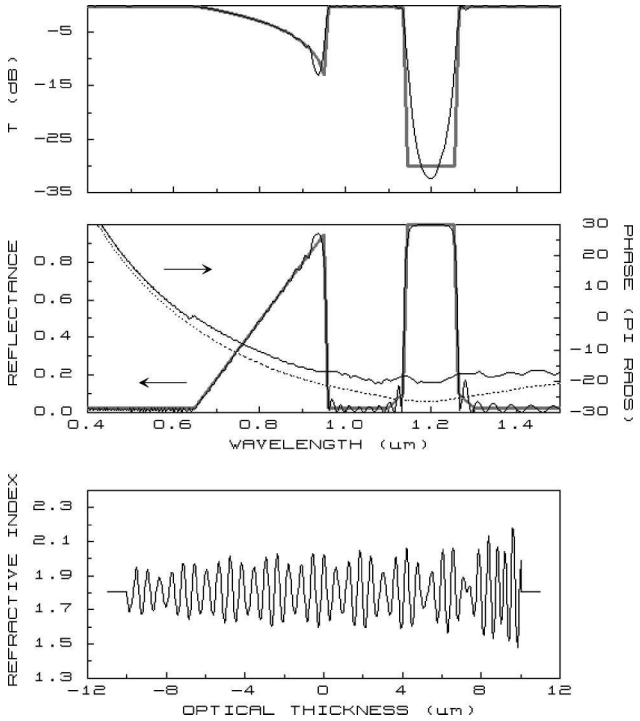

Fig. 2. Result of the SWIFT phase optimization. The starting and final phases are represented by a dashed and a solid black line, respectively. The upper part of the figure is the transmittance in decibels $[10\log(T)]$.

curvature spreads the index profile along the thickness axis and is responsible for the reduced index modulation. The excess modulation is shifted out of the allowed thickness range and simply ignored. To illustrate this, the rugate is recalculated over a wider thickness range in Fig. 3. The same complex Q function (magnitude and phase) is used in the Fourier transforms. The central part of the system is the previous design obtained when the shaded regions are ignored.

The contribution of each reflectance band to the overall refractive-index profile can be identified by Fourier analysis [19,20]. Figure 4 illustrates the result. The respective index contributions are found by taking the inverse Fourier transform of the index profile and transforming back each half of the spectrum separately (wavelengths $>$ and $<1.05\,\mu$m, respectively). The index contribution of the 2nd reflectance band is essentially a wavelet (apodized

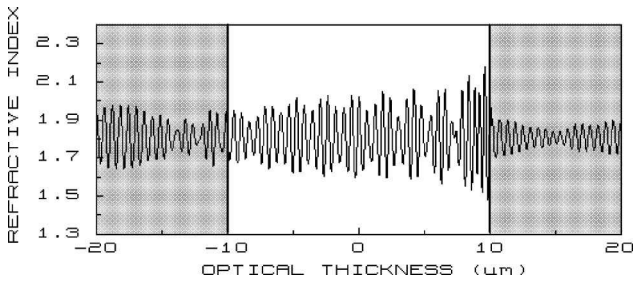

Fig. 3. Previous design recalculated over a wider thickness range. The shaded regions are ignored in Fig. 2.

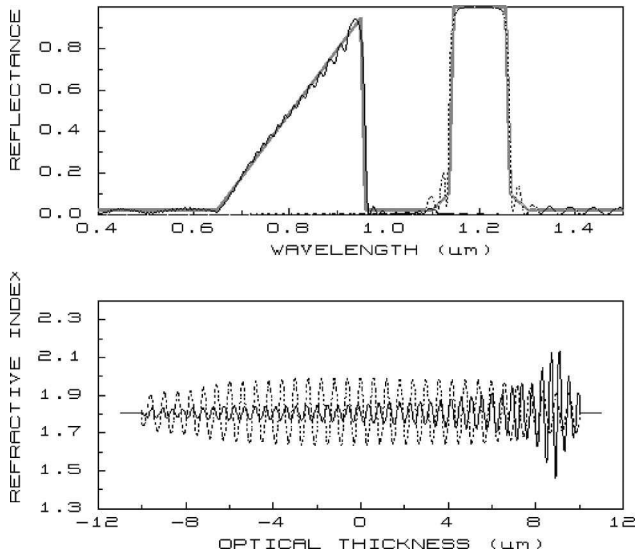

Fig. 4. Fourier analysis of the design shown in Fig. 2. The solid and dashed black lines represent the refractive-index modulation corresponding to the 1st and 2nd reflectance bands, respectively, and their reflectance. The dashed index profile is essentially a wavelet.

sinusoid [21]) spread over the whole available thickness. The contribution of the triangular band is mostly concentrated on the right-hand side of the system. This configuration minimizes the index overlap but does not eliminate it completely. The refractive-index beats visible in Fig. 2 correlate with the degree of overlap. Note that the reflectance of the two sub systems is remarkably accurate, in spite of the high-reflectance limitations of the conventional FT approach [20].

It is interesting that the results of the phase optimization are quite insensitive to the accuracy of $Q(T)$. Figure 5 illustrates a solution obtained with [1,9,16]

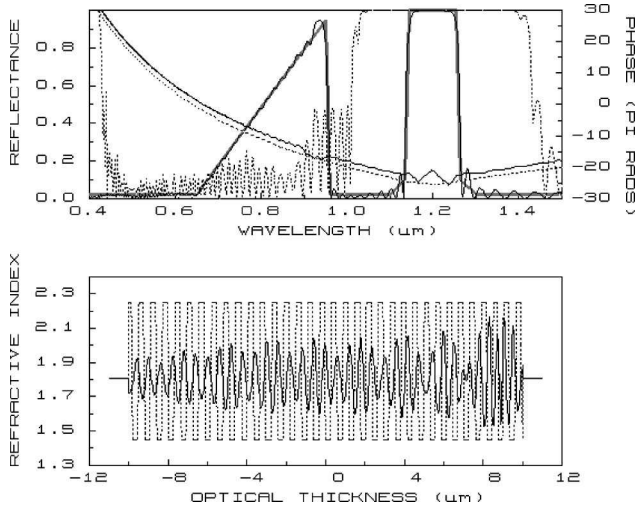

Fig. 5. Result obtained with a different form of the Q-function magnitude [Eq. (5)]: dashed lines, SWIFT phase and starting design; solid lines, result after phase optimization.

$$Q(T) = \sqrt{\frac{R}{T}}. \tag{5}$$

This is one of the early published forms of $Q(T)$, which typically leads to a large overshoot of the target reflectance. The starting design generated by the plotted SWIFT phase is represented by dashed lines. The refractive-index modulation is much too large and must be clipped at the index limits. The fit of the calculated reflectance with the target is very poor. Nevertheless, the phase optimization is still able to produce a good result represented by solid black lines. The refractive-index profile and its reflectance are almost the same as in Fig. 2. The optimized phase is different, in particular across the 2nd reflectance band.

Several other published forms of $Q(T)$ produced similar results. The key point is that the reflectance of the starting design must be high enough because it is reduced (on average) when the system is stretched and clipped at the prescribed thickness and index limits. Some forms of $Q(T)$ do not generate enough reflectance, for example, $Q(T) = \sqrt{1-T} = \sqrt{R}$.

For simplicity, the previous designs were immersed in a medium of average index. Asymmetrical media are also possible. One way to achieve this is to multiply the immersed design by a fixed, slowly varying index. When the variation is slow enough, reflectance is added only at low wavenumbers outside the region of interest. An abrupt index step, e.g., at an air interface, increases the reflectance across the whole spectrum. An example of slowly varying index terminated by an abrupt step is represented by a dashed line in Fig. 6. The substrate is semi-infinite glass (backside reflections are ignored) and the ambient medium is air. The filter is assumed to be a dispersive mixture of Nb_2O_5 and SiO_2. Material dispersion is introduced when the reflectance of the FT design is calculated; the Fourier transforms themselves are nondispersive [4–7,20]. For compatibility with the previous examples, the target reflectance is changed to the reflectance of the bare substrate or less (<4%) in the transmitting regions. Otherwise, the substrate has to be antireflected and this introduces homogeneous layers. The final result is still good in spite of the additional requests.

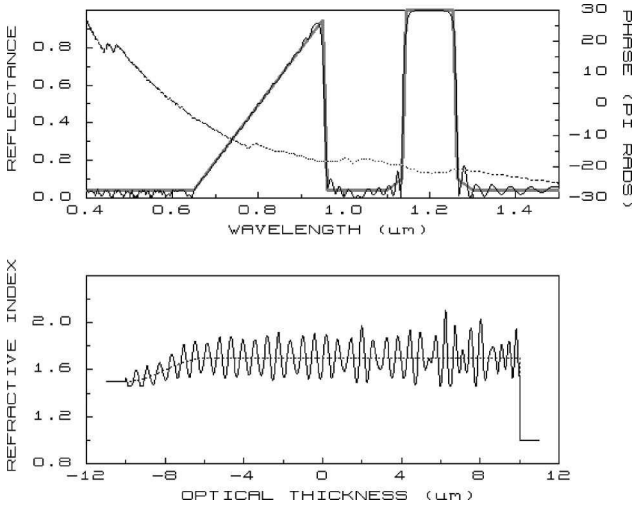

Fig. 6. Fourier transform design of a rugate reflector on a semi-infinite glass substrate in air. The filter is assumed to be a mixture of SiO_2 and Nb_2O_5. Material dispersion is included.

Finally, a more difficult example can be seen in the design of a filter simulating the silhouette of the Taj Mahal, as illustrated in Fig. 7. Several rugate and multilayer versions of this filter have been published as a demonstration of design and manufacturing capabilities. For simplicity, material dispersion is ignored in the present calculation. The result of the phase optimization compares well with the previous examples and with published Taj Mahal filter designs [20,22]. The SWIFT phase is recognizable in the central part of the building but significantly modified elsewhere. In particular, it is almost flat across the thin towers to keep their index contribution in the available thickness space.

The spectral performance of the previous designs is not much improved when the synthesis is continued with more accurate techniques. For example, one could refine the full complex Q function (magnitude and phase) or even the refractive indices [20]. The improvements are quickly at the expense of refractive-index smoothness. Thin layers of high index contrast appear at the outer interfaces and slowly spread in the system. This is typical in the later stages of rugate filter synthesis. It is well known that at normal incidence the optimum thin film designs are composed of two materials of the highest possible index ratio. The phase shaping procedure automatically preserves the index smoothness because $Q(T)$ is fixed and assumed to be zero outside the spectral region of interest (no high frequencies are generated). The control of index smoothness is a key in rugate filter synthesis and is also useful when they are converted in multilayers because this limits the proliferation of thin layers.

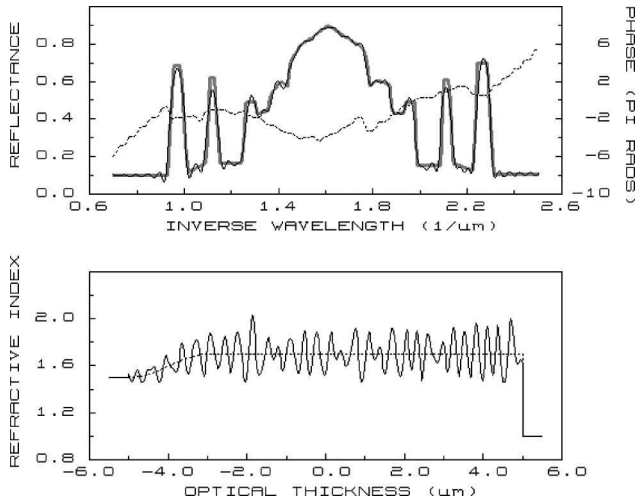

Fig. 7. Fourier transform design of a rugate filter corresponding to the silhouette of the Taj Mahal.

4. Conclusions

This work clearly confirms the importance of the phase in thin film synthesis by Fourier transforms and demonstrates that surprisingly good rugate reflector designs can be generated by phase shaping alone. The phase belongs to the spectral function that is Fourier transformed (the Q function, a function of the desired spectral characteristics). Usually the approach is the reverse; namely, the focus is on the magnitude of the Q function while its phase is of secondary concern.

The operating mode of this design approach is quite unusual and interesting in itself. The phase is used to stretch the synthesized refractive-index profile along the thickness axis. The index variations that end up outside predetermined thickness limits are simply ignored. The Q-function magnitude is not varied and its accuracy is not critical as long as it generates enough reflectance. Refractive-index smoothness is automatically preserved, a useful asset in rugate filter synthesis.

A related approach exists in laser pulse shaping, but the implementation is different and the accuracy of the fit (pulse height) is less important [23]. A preliminary version of this work was presented at the 2010 Optical Interference Coatings Topical Meeting [24].

References

1. E. Delano, "Fourier synthesis of multilayer filters," J. Opt. Soc. Am. **57**, 1529–1532 (1967).
2. L. Sossi, "A method for the synthesis of multilayer dielectric interference coatings," Eesti NSV Tead. Akad. Toim. Fuus. Mat. **23**, 229–237 (1974). An English translation is available from the Translation Services of the Canada Institute for Scientific and Technical Information, National Research Council of Canada, Ottawa, Ontario, Canada KlA 0R6.
3. J. A. Dobrowolski and D. Lowe, "Optical thin film synthesis program based on the use of Fourier transforms," Appl. Opt. **17**, 3039–3050 (1978).
4. H. Fabricius, "Gradient-index filters: conversion into a two-index solution by taking into account dispersion," Appl. Opt. **31**, 5216–5220 (1992).
5. P. V. Bulkin, P. L. Swart, and B. M. Lacquet, "Fourier-transform design and electron cyclotron resonance plasma-enhanced deposition of lossy graded-index optical coatings," Appl. Opt. **35**, 4413–4419 (1996).
6. D. Poitras, S. Larouche, and L. Martinu, "Design and plasma deposition of dispersion-corrected multiband rugate filters," Appl. Opt. **41**, 5249–5255 (2002).
7. S. Larouche and L. Martinu, "Dispersion implementation in optical filter design by the Fourier transform method using correction factors," Appl. Opt. **46**, 7436–7441 (2007).
8. B. G. Bovard, "Fourier transform technique applied to quarterwave optical coatings," Appl. Opt. **27**, 3062–3063 (1988).
9. P. G. Verly, J. A. Dobrowolski, W. J. Wild, and R. L. Burton, "Synthesis of high rejection filters with the Fourier transform method," Appl. Opt. **28**, 2864–2875 (1989).
10. W. J. Wild, "Analytic improvement of Sossi's Q function," Appl. Opt. **28**, 3272–3273 (1989).
11. P. G. Verly and J. A. Dobrowolski, "Iterative correction process for optical thin film synthesis with the Fourier transform method," Appl. Opt. **29**, 3672–3684 (1990).
12. P. G. Verly, "Fourier transform technique with refinement in the frequency domain for the synthesis of optical thin films," Appl. Opt. **35**, 5148–5154 (1996).
13. X. Cheng, B. Fan, J. A. Dobrowolski, L. Wang, and Z. Wang, "Gradient-index optical filter synthesis with controllable and predictable refractive index profiles," Opt. Express **16**, 2315–2321 (2008).
14. R. Szipocs and A. Kohazi-Kis, "Theory and design of chirped dielectric laser mirrors," Appl. Phys. B **65**, 115–135 (1997).
15. P. G. Verly, A. V. Tikhonravov, and A. D. Poezd, "Multiple solutions to the synthesis of graded index optical coatings," Proc. SPIE **2046**, 9–16 (1993) .
16. A. V. Tikhonravov, "Some theoretical aspects of thin-film optics and their applications," Appl. Opt. **32**, 5417–5426 (1993).
17. J. Druessel, J. Grantham, and P. Haaland, "Optimal phase modulation for gradient-index optical filters," Opt. Lett. **18**, 1583–1585 (1993).
18. P. G. Verly, A. V. Tikhonravov, and M. K. Trubetskov, "Efficient refinement algorithm for the synthesis of inhomogeneous optical coatings," Appl. Opt. **36**, 1487–1495 (1997).
19. P. G. Verly, "Fourier transform technique with frequency filtering for optical thin-film design," Appl. Opt. **34**, 688–694 (1995).
20. P. G. Verly, "Hybrid approach for rugate filter design," Appl. Opt. **47**, C172–C178 (2007).
21. W. H. Southwell, R. L. Hall, and W. J. Gunning III, "Using wavelets to design gradient-index interference coatings," Proc. SPIE **2046**, 46–59 (1993).
22. P. G. Verly, "Design of inhomogeneous and quasi-inhomogeneous optical coatings at the NRC," Proc. SPIE **2046**, 36–45 (1993).
23. M. Hacker, G. Stobrawa, and T. Feurer, "Iterative Fourier transform algorithm for phase-only pulse shaping," Opt. Express **9**, 191–199 (2001).
24. P. G. Verly, "Optimum phase for thin film synthesis by Fourier transforms," in *Optical Interference Coatings on CD-ROM* (The Optical Society of America, 2010), pp. TuB2 1-3.